

VICTORIA UNIVERSITY
MELBOURNE AUSTRALIA

Scalable production of hydroxyl radicals ($\cdot\text{OH}$) via homogeneous photolysis of hydrogen peroxide using a continuous-flow photoreactor

This is the Accepted version of the following publication

Mahbub, Parvez, Smallridge, Andrew, Irtassam, Asjid and Yeager, Thomas (2021) Scalable production of hydroxyl radicals ($\cdot\text{OH}$) via homogeneous photolysis of hydrogen peroxide using a continuous-flow photoreactor. *Chemical Engineering Journal*, 427. ISSN 1385-8947

The publisher's official version can be found at
<https://www.sciencedirect.com/science/article/abs/pii/S138589472103343X?via%3Dihub>
Note that access to this version may require subscription.

Downloaded from VU Research Repository <https://vuir.vu.edu.au/42506/>

Journal Pre-proofs

Scalable production of hydroxyl radicals ($\cdot\text{OH}$) via homogeneous photolysis of hydrogen peroxide using a continuous-flow photoreactor

Parvez Mahbub, Andrew Smallridge, Asjid Irtassam, Thomas Yeager

PII: S1385-8947(21)03343-X
DOI: <https://doi.org/10.1016/j.cej.2021.131762>
Reference: CEJ 131762

To appear in: *Chemical Engineering Journal*

Received Date: 29 June 2021
Revised Date: 4 August 2021
Accepted Date: 6 August 2021



Please cite this article as: P. Mahbub, A. Smallridge, A. Irtassam, T. Yeager, Scalable production of hydroxyl radicals ($\cdot\text{OH}$) via homogeneous photolysis of hydrogen peroxide using a continuous-flow photoreactor, *Chemical Engineering Journal* (2021), doi: <https://doi.org/10.1016/j.cej.2021.131762>

This is a PDF file of an article that has undergone enhancements after acceptance, such as the addition of a cover page and metadata, and formatting for readability, but it is not yet the definitive version of record. This version will undergo additional copyediting, typesetting and review before it is published in its final form, but we are providing this version to give early visibility of the article. Please note that, during the production process, errors may be discovered which could affect the content, and all legal disclaimers that apply to the journal pertain.

© 2021 Elsevier B.V. All rights reserved.

Scalable production of hydroxyl radicals ($\cdot\text{OH}$) via homogeneous photolysis of hydrogen peroxide using a continuous-flow photoreactor

Parvez Mahbub*¹, Andrew Smallridge^{1,2}, Asjid Irtassam¹ Thomas Yeager^{1,2}

¹Institute for Sustainable Industries and Liveable Cities (ISILC), Victoria University, Footscray Park Campus, Melbourne 3011, Australia

²First Year College, Victoria University, Footscray Park Campus, Melbourne 3011, Australia

* Corresponding Author Email: parvez.mahbub@vu.edu.au

Abstract

We establish the fact that in a continuous-flow scalable photoreactor system employed for the homogeneous photolysis of H_2O_2 into $\cdot\text{OH}$ radicals, the quantum yield of photolytic conversion in aqueous solution cannot be regarded as a linear function of H_2O_2 initial concentration. We were successful in repeatedly producing high concentrations of $\cdot\text{OH}$ radical (between 40 – 90 mM) from relatively low concentrations of hydrogen peroxide (between 0.1 M - 5 M) in aqueous solution in a scalable manner using our serially connected photoreactor system. Our investigation demonstrates that merely selecting a very high initial concentration of H_2O_2 will not necessarily result in the highest conversion into $\cdot\text{OH}$ radical. We also developed a simple and *in-situ* acid-base titrimetric method for quantitation of $\cdot\text{OH}$ radicals and demonstrated an accuracy of our method within $\sim\pm 6.6\%$

of a ^{31}P NMR method. Hence, our proposed scalable $\cdot\text{OH}$ radical production method via continuous-flow photoreactors can be regarded as a safe, simple, accurate and cost-effective technique for various industrial processes, particularly in aquaculture and swimming pool disinfection, as a replacement of high concentrations of hazardous oxidisers.

Keywords: continuous-flow scalable photoreactor, photolysis of hydrogen peroxide (H_2O_2), *in-situ* quantitation of hydroxyl ($\cdot\text{OH}$) radicals

1. Introduction

The hydroxyl radical ($\cdot\text{OH}$) is one of the most reactive radical species affecting living systems [1,2].

$\cdot\text{OH}$ radicals with half-life of 10^{-10} s or 0.1 ns [3], interact directly with organic and inorganic substances in living systems via rapid exchange of unpaired electrons [4, 5]. Due to very fast reactivity towards living organisms, $\cdot\text{OH}$ is a potent candidate for deactivating hazardous microorganisms in aqueous media [6]. There are a number of reports of application of $\cdot\text{OH}$ radicals, generated via various advanced oxidation processes (AOPs), in the remediation of hazardous microorganisms particularly in aqueous media [7, 8]. The AOPs include UV+ozone (O_3), UV+hydrogen peroxide (H_2O_2), Fenton, photo-Fenton, nonthermal plasmas, sonolysis, photocatalysis, radiolysis, and supercritical water oxidation processes [9]. Aside from some intermediate by-products, $\cdot\text{OH}$ radicals are the main reaction product in almost all of these AOPs.

The application of $\cdot\text{OH}$, generated via advanced oxidation processes (AOPs) in large industry-scale, is dependent on simplicity of up and/or down-scaling techniques of $\cdot\text{OH}$ radical production, cost of energy and reagent (such as, oxidisers and catalysts) usage, as well as on the rapid and accurate *in-situ* measurement techniques of $\cdot\text{OH}$ radicals in high concentrations. The lack of scalability in $\cdot\text{OH}$ radical production as per demand, high reagent cost during AOP operations and the lack of capability of accurate measurement of $\cdot\text{OH}$ radicals *in-situ* are the existing capability gaps in industrial utilisation of $\cdot\text{OH}$ radicals.

Hydrogen peroxide is the most readily available and commercially viable material to produce $\cdot\text{OH}$ radicals via AOP. Photolysis of H_2O_2 via homogeneous [10-13] or heterogeneous [14] catalytic or non-catalytic processes in either batch mode (almost all of the published reports) or continuous-flow

modes (scarcely reported to date) were employed to produce $\cdot\text{OH}$ radicals for various organic and inorganic contaminants' degradation in liquid media. In this context, the continuous-flow mode of non-catalytic homogeneous photolysis of H_2O_2 is particularly interesting as this technique can readily adopt upscaling or downscaling of photo-production of $\cdot\text{OH}$ without the need for any soluble/insoluble photocatalyst, promoters or photosensitisers in the system, thus reducing the production cost of the $\cdot\text{OH}$ radicals for industrial use. Although semiconductor based heterogeneous photolysis of H_2O_2 in batch mode results in high quantum yield (QY) (i.e., mole of product reacted/mole of photon absorbed) compared to the non-catalytic homogeneous photolysis of H_2O_2 , the actual production yield (PY) in terms of product formed can be easily controlled and reproduced via direct homogeneous photolysis of H_2O_2 in continuous-flow conditions [15], thus resulting in significant economic benefits in industrial operations involving radicals. Additionally, continuous-flow mode of reactor operations ensure the continuous supply of very 'short-lived' radicals in aqueous solutions as opposed to the batch mode where effective radical concentrations may attenuate significantly before their intended use.

For the detection of $\cdot\text{OH}$, primarily as adducts in various matrices, numerous detection systems have been employed, such as electrochemical (EC) detection systems including cyclic voltammetry [16-22] and amperometry [23, 24], photometric detection systems such as UV detection [24], fluorescence [25], chemiluminescence [26, 27] as well as spectroscopic systems such as electron spin resonance (ESR) [4] and resonance scattering (RS) [28]. These methods require specific reagents and/or complex derivatization processes, which usually trap the $\cdot\text{OH}$ to form stable adducts before subsequent detection and quantification of $\cdot\text{OH}$. The common limitation of all of these $\cdot\text{OH}$ detection techniques is the non-linearity of the detection at concentrations in high millimolar or molar ranges and their inability to be employed *in-situ*. Large industrial processes require to scale-up or scale-

down the $\cdot\text{OH}$ production regularly on the basis of demand which will require a reliable, accurate and scalable *in-situ* $\cdot\text{OH}$ detection system suitable for the field. In this regard, Steiner and Babbs [29] demonstrated dimethyl sulfoxide (DMSO) based spectroscopic method for quantitation of $\cdot\text{OH}$ radicals generated via Fenton reaction, gamma radiolysis of water as well as via direct homogeneous photolysis of H_2O_2 . Their method was based on the reaction of $\cdot\text{OH}$ with DMSO producing methanesulfonic acid (MSA) and methyl radical. The MSA was measured by a diazonium salt based colorimetric assay [30] within a restricted range of 30 to 300 μM MSA via visible absorption spectroscopy. Potentiometric titration of MSA crystals using glass electrodes was first reported by Wudl et al. [31]. In this regard, we propose direct acid-base titration of MSA in aqueous solution using strong bases such as NaOH in presence of phenolphthalein which can be a simple, accurate, cost effective and readily scalable *in-situ* MSA measurement approach particularly when high millimolar or molar concentrations of MSA derived from the reaction between $\cdot\text{OH}$ and DMSO is anticipated. Therefore, in our investigation, we demonstrate a rapid *in-situ* measurement technique of $\cdot\text{OH}$ radical at high concentrations via simple acid-base titration of MSA formed during the reaction between $\cdot\text{OH}$ and DMSO in aqueous solution, enabling the upscaling and downscaling of industrial scale production of $\cdot\text{OH}$ radical via direct homogeneous photolysis of H_2O_2 , and discuss its potential applications. We also demonstrate the verification of our *in-situ* $\cdot\text{OH}$ measurement by comparing our results with well-established ^{31}P based nuclear magnetic resonance (^{31}P NMR) method of $\cdot\text{OH}$ quantitation [32].

2. Materials and methods

2.1 Chemicals and consumables

Analytical grade chemicals were used in this study. 30% (w/w) H_2O_2 (product code 216763-500 mL) was purchased from Sigma Aldrich Australia. The proposed acid-base titration method of MSA for

the quantitation of $\cdot\text{OH}$ in this study was verified by nuclear magnetic resonance (NMR) based standard method of $\cdot\text{OH}$ radical measurement published earlier [32]. The NMR reagents such as diethylenetriaminepentaacetic acid (DTPA $\geq 99\%$; product code D6518-5G), NMR internal standard trimethyl phosphate (TMP $\geq 99\%$; product code 241024-50G), spin relaxation agent chromium (III) chloride and Wilmad[®] NMR tubes (product code Z562769-5EA) were purchased from Sigma-Aldrich Australia. The NMR spin trapping agent 5-diisopropoxy-phosphoryl-5-methyl-1-pyrroline-N-oxide (DIPPMPO; product code ALX-430-119-M050) was purchased from United Bioreserch Australia. The fluoroethylene polymer (FEP; part no 1677L) tubings and accesories to construct the photoreactor were purchased from IDEX Health and Science USA. Phenolphthalein and sodium hydroxide pellets, potassium permanganate and 98% (w/w) sulphuric acid were also purchased from Sigma Aldrich Australia. Standard titration bench was used to titrate MSA with 0.001 M NaOH using the phenolphthalein indicator. We also used 0.1M potassium permanganate to titrate 30% (w/w) H_2O_2 . Please refer to the supplementary information (SI) for details of these titration methods.

2.2 Instrumentations

G6T5N UV-C medium pressure mercury lamp (210 mm length; 15 mm nominal diameter) was purchased from Australian Ultraviolet Services Pty Ltd. The FEP tubes were coiled around the lamps in either 1, 2, 3 or 4 layers demonstrated later in section 3.1. For fluid propulsion, we used Varian Prostar (model 215) solvent delivery pump. The schematic representation of the scalable reactor system is shown in Figure 1.

Insert Figure 1

2.3 ^{31}P NMR experiments

The ^{31}P NMR spectra were recorded using a Bruker-600 instrument operating at 242.9MHz. All spectra were recorded with ^1H decoupling, 256 scans with an acquisition time of 1.7s and a delay of

2s (5 x 400 ms relaxation time T_1 as reported by Argyropoulos et al. [32]. The chemical shifts reported are relative to external orthophosphoric acid (85%). Trimethyl phosphate was used as the internal standard for quantification and was added to the sample prior to measurement. The samples were prepared by adding 200 μL of sample to 200 μL of D_2O and 100 μL of CrCl_3 as a relaxation agent.

3. Results and Discussions

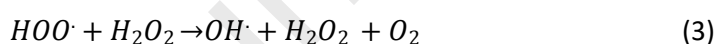
3.1 Scalable production of $\cdot\text{OH}$ radical

The construction of the scalable photoreactor to photolyse hydrogen peroxide into radicals and their subsequent quantitation was the primary step of our investigation. Aside from the intermediate reaction by-products, the photo degradation products of H_2O_2 in aqueous solutions is mainly $\cdot\text{OH}$ radical as reported by Liao and Gurol [33]:

Initiation/light absorption



Propagation



Termination



Unlike forming $\cdot\text{OH}$ adducts by the $\cdot\text{OH}$ radical trapping agents such as, 5-diisopropoxy-phosphoryl-5-methyl-1-pyrroline-N-oxide (DIPPMPO), used in nuclear magnetic resonance (NMR) spectroscopy, dimethyl sulfoxide (DMSO) readily gets oxidised by the $\cdot\text{OH}$ radical to produce methane sulfinic acid (MSA) as per the following reaction [29]:



Our proposed $\cdot OH$ radical measurement technique is based on weak acid - strong base titration of methane sulfinic acid (MSA) in aqueous solution using NaOH in presence of phenolphthalein as an indicator of reaction end-point which is determined at the occurrence of consistent pale pink colour indicating precipitation of sodium methanesulfinate salt.



From the last two balanced equations, we observe that the number of mole of sodium hydroxide required to achieve the titration end-point with MSA in equation 6 is actually equal to the number of mole of $\cdot OH$ radical reacted with DMSO in equation 5. Hence, measuring the concentration of MSA in equation 5 should give the concentration of $\cdot OH$ radicals in the system which was employed to oxidise DMSO. In this investigation, we worked with concentrated H_2O_2 . The molarity of 30% (w/w) H_2O_2 equates to 9.7898 M H_2O_2 in aqueous solution at room temperature of 20 °C. Although there are a number of titration methods reported for the quantitation of high molar concentration of H_2O_2 (e.g., dichromate and cerium sulphate titrations), the permanganate based titration provides accurate quantitation of high molar ranges without the need for any limiting agents or indicators. The detailed steps of both H_2O_2 and our proposed $\cdot OH$ measurement techniques are given in supplementary information (SI) section.

The photoreactor was constructed with four reactors connected in series. Each reactor consisted of a 21cm long G6T5N Hg lamp wrapped around by 2 mm internal diameter (I.D.) FEP tubing ranging from 1 layer to 4 layers of tubing as shown in Figure 2.

Insert Figure 2

The G6T5N UV lamps are rated for 6-watt electrical energy consumption per lamp. Therefore, for a serially connected reactor arrangement as shown in Figs.2a and 2b, the total electrical energy

consumption per reactor would be 24 watts. If multiple reactors are connected in parallel as per industrial needs, then the electrical energy consumption would increase accordingly. The UV radiometric output of G6T5 lamp is rated as 1.7 watts per lamp, which makes the overall energy efficiency (i.e., radiometric energy output/electrical energy input x 100) of a single reactor as ~28%. We employed different initial concentrations of hydrogen peroxide ranging from 10.48 M to 0.1 M H_2O_2 with a combination of layers of either 1, or 2, or 3, or 4, or 3+2, or 3+2+1, or 4+3+2+1 as shown in Table 1. The flowrate and DMSO concentrations were maintained constant at 20 mL/min and 0.8 M, respectively. Each run continued for about 1 min to 6 min depending on the layer numbers of the reactor and we collected the product at the outlet for subsequent measurement of 'H₂O₂ remaining' and 'OH radical produced' during photolysis using the two titration-based simple methods described in the SI.

Insert Table 1

The variation of OH radical production and the initial concentration of H_2O_2 is not explicit in Table 1. Hence, we plotted the initial concentration of H_2O_2 against the OH radical produced only for a serially connected photoreactor system (i.e., layers 4+3+2+1) as shown in Figures 3A.

Insert Figure 3A

In Figure 3A, we observe an inverse relationship between OH radical produced and actual H_2O_2 spent in the photolytic process where the OH production reached at a peak of ~83 mM when initial concentration of H_2O_2 was only 0.5 M and ~55 mM of this initial H_2O_2 was spent to produce ~83 mM OH radical. The quantum yield of photolytic conversion of hydrogen peroxide to OH radical has been reported as reciprocally dependent on the square root of the intensity of the absorbed radiation according to the following equation [34]:

$$\varphi = 2k_1 + 2k_5 \sqrt{\frac{k_1}{k_7 I}} [H_2O_2] \quad (7),$$

where $K_1 - K_7$ are the reaction kinetic coefficients of intermediate reactions and I is light intensity. Luňák and Sedlák [34] noted the relatively narrow range of reaction conditions within which the linearity of equation 7 was verified, raising the question of whether the results of equation 7 can confirm the photolysis of H_2O_2 in all conditions. Another much earlier study by Heidt [35] demonstrated reduction of the quanta absorbed with increased concentration of H_2O_2 at constant light intensity and time of photolysis (7.2×10^{-3} sec) in aqueous solution with acidic pH. In our observation in Figure 3A, although there was an increase in $\cdot OH$ radical concentrations from 0.1 M to 0.5 M initial H_2O_2 concentration, the $\cdot OH$ radical production gradually decreased with further increase of H_2O_2 concentration beyond 0.5 M. This reaffirms the scepticism of Luňák and Sedlák [34] regarding the linearity of equation 7 for a narrow range of experimental condition. As we maintained a constant flowrate of 20 mL/min with a precise HPLC pump, and the volume and internal geometry of the reactor remained unchanged throughout the experiment, the optical path-length should remain constant in our experiment. We attribute the non-linearity of quantum yield of photolysis of H_2O_2 towards varying initial concentration and pH of the solution. An important fact to be noted is that only a small portion of the initial concentration of H_2O_2 was spent to produce $\cdot OH$ radical in our continuous-flow photoreactor. For example, in Figure 3A, we observe that only 1.9 M out of 5 M H_2O_2 was used to produce the 55 mM $\cdot OH$ radical. We investigated whether the similar trend in the $\cdot OH$ radical production with varying initial concentrations of H_2O_2 can be observed for other arrangements of the serially connected layers of the photoreactor (e.g., 3+2+1 layers) as shown in Figure 3B.

Insert Figure 3B

Although not as explicit as in Figure 3A, we observe that a similar trend of $\cdot\text{OH}$ radical production related to the varying concentrations of H_2O_2 from 10.18 M to 5 M in Figure 3B at a constant flowrate of 20 mL/min. We attribute the observed trend of photo-conversion of H_2O_2 into $\cdot\text{OH}$ radicals as an intrinsic property (i.e, internal geometry and optical pathlength) of our serially connected continuous-flow photoreactor. In this context, the non-linear regime of the famous Beer-Lambert law of photo-absorption of molecules [36] in terms of high concentrations of H_2O_2 causing electrostatic interactions amongst molecules in close proximity as well as scattering of light due to presence of particulates in the aqueous sample might have played significant roles in addition to the pH of the solution during the photolytic conversion of H_2O_2 into $\cdot\text{OH}$ radicals using our proposed reactors. We also observe in Table 1 that stand-alone layers of the reactor (i.e., either 1, or 2, or 3, or 4) were able to produce $\cdot\text{OH}$ radicals in the range of 10 mM to 30 mM at a constant flowrate of 20 mL/min, irrespective of the initial concentrations of H_2O_2 . The conversion of H_2O_2 into $\cdot\text{OH}$ radicals gradually increased at constant flowrate of 20 mL/min and constant initial concentration of 10.48 M from 20 mM in layer 1 to ~ 50 mM in layers 3+2+1. Therefore, merely selecting a very high initial concentration of 10.48 M H_2O_2 will not necessarily result in highest conversion into $\cdot\text{OH}$ radical. This observation forms the basis of scalability of the proposed photoreactor system. Depending on the demand of $\cdot\text{OH}$ radicals in an industrial process, our proposed photoreactor system can be adjusted in terms of either stand-alone layers (i.e., either 1, or 2, or 3, or 4) or serially connected layers (i.e., either 3+2, or 3+2+1, or 4+3+2+1). Another important fact in both cases of Figures 3A and 3B to be noted is that the concentrations of H_2O_2 converting to $\cdot\text{OH}$ radicals were significantly lower than the initial concentrations of H_2O_2 used in the system. Therefore, the selection of a suitably low concentration of H_2O_2 that results in maximum $\cdot\text{OH}$ radical conversions at the minimal usage of H_2O_2 using our scalable photoreactor system will have an impact on reduced operational cost of using H_2O_2 as a reagent in industrial processes. We repeated the same set of experiment in Fig. 3A three

months apart for the 4+3+2+1 reactor arrangement, and observed that the conversion efficiency of reactor (i.e., $\cdot\text{OH}$ produced/initial concentration of H_2O_2 used) remained relatively stable over the period, with maximum 90 mM $\cdot\text{OH}$ radicals were produced again from 0.5 M H_2O_2 at a conversion efficiency of $\sim 18\%$ (Table S1 in supplementary information). The stability of conversion efficiency of the reactor will primarily depend on the level of use of the reactor. In this context, the *in-situ* manner of $\cdot\text{OH}$ radical measurement using our proposed titrimetric method facilitates a simple, portable and rapid means of checking the conversion efficiency of the reactor at reasonable time intervals.

3.2 Verification of in-situ $\cdot\text{OH}$ Radicals Detection Method

We compared our simple $\cdot\text{OH}$ radical measurement technique based on acid-base titration of MSA produced from the reaction between $\cdot\text{OH}$ radical and DMSO with a previously established $\cdot\text{OH}$ radical measurement technique based on radical trapping by a nitroxide phosphorus compound (DIPPMPO) reported by Argyropoulos et al. [32].

50 mL solutions containing 140 μM H_2O_2 and 3.8 mM DMSO were prepared and injected into the single layer photoreactor in a continuous-flow mode at a flowrate of 20 mL/min (sample set A). We also prepared 50 mL solutions containing 140 μM H_2O_2 and 3.8 mM DIPPMPO and 2.54 mM DTPA as metal chelating agent as suggested by Argyropoulos et al.[32] and then injected into the single layer photoreactor in a continuous-flow mode at a flowrate of 20 mL/min (Sample set B). The samples were collected after approximately 1 min 25 sec waiting period in both cases. The *in-situ* titration was readily employed on sample set A, whilst the sample volume of set B was precisely measured for the NMR analyses. We then added trimethylphosphate (TMP) as internal standard (I.S.) into sample set B so that the final TMP concentration in sample set B becomes 2.42 mM. Prior to NMR

analyses, we also added 0.1 mL 821 μM CrCl_3 as spin relaxation agent into the NMR tubes. Table 2 shows $\cdot\text{OH}$ radical concentrations in sample sets A and B via the titration and NMR, respectively.

Insert Table 2

In Table 2, we observe that there is an excellent similarity (Average: via titration = 1.08 mM compared to via NMR = 1.0128 mM, i.e., titrations were within $\pm 6.6\%$ accuracy of NMR) between the $\cdot\text{OH}$ radical concentrations achieved via our *in-situ* titration method and the established NMR method.

The chemical shift of DIPPMO-OH adduct was 25.3 ppm and that of DIPPMPPO was 22.2 ppm as reported by Argyropoulos et al.[32]. These reported shifts are almost identical to our findings as shown in Figure 4 for DIPPMO-OH adduct as well as for DIPPMPPO. Two more major peaks as radical intermediate adduct at 18.3 ppm and as DIPPMPPO-OOH adduct at 17.1 ppm were reported in their study. As the photolysis of H_2O_2 produces $\cdot\text{OH}$ radical, $\cdot\text{OOH}$ radical, superoxide anion radical (O_2^-) as well as molecular oxygen (O_2) at various stages of photolysis (eqn. 1-4), we also attribute our remaining peak in Figure 4 at 10.87 ppm as 'radical intermediate adducts with DIPPMPPO'. We repeated our NMR analyses for 5 consecutive times (each time preparing a new sample set B) which resulted almost reproducible $\cdot\text{OH}$ radical concentrations and corresponding chemical shifts of DIPPMPPO-OH adducts. The NMR results and NMR experimental conditions are provided in SI.

Insert Figure 4

3.3 Comparative Study of $\cdot\text{OH}$ radical production Systems

Through our investigation, we have demonstrated an accurate and simple technique to produce high concentrations (millimolar to molar ranges) of $\cdot\text{OH}$ radicals via continuous-flow photoreactors intended for large scale use. To the contrary, all the existing work published on the $\cdot\text{OH}$ radicals to

date are mainly focussed on its trace detection (in nano to micromolar scale as shown in Table 3) rather than accurately measuring high $\cdot\text{OH}$ radical concentrations ranges. Additionally, the $\cdot\text{OH}$ radicals' productions were achieved through batch mode in almost all published reports to date (Table 3).

Insert Table 3

As our proposed titrimetric method is a simple, portable, small, inexpensive and energy efficient method compared to NMR, resonance scattering or hydroxylation methods in Table 3, we termed this as an *in-situ* method in the sense that the whole analysis can be performed at the field location using the reactor without compromising the fast decay of $\cdot\text{OH}$ radicals. In this context, another comparable *in-situ* method is the DNA-based electrochemical biosensing [21], however, this study did not report on scalability of $\cdot\text{OH}$ radical production.

4. Potential Application of Scalable $\cdot\text{OH}$ Radical Production

Salmon aquaculture is a significant industry in Australia. Amoebic Gill Disease (AGD) caused by a parasite known as *Neoparamoeba perurans* is one of the major problems that affect the salmon industries in Australia and around the globe. Freshwater bathing of Atlantic salmon for 2-3 hr is the current recommended treatment of AGD [37]. The key challenges in salmon-bathing technique are: re-use of freshwater, recurrence of the amoebic gill disease (AGD) after initial bathing, and the long fish-bathing time of 2-3 hr. Recently, Mahbub and Sharma [38] reported monthly and daily freshwater demand for salmon-bathing in the range of 120 megalitres (ML)/month and 2 ML/day, respectively by medium-sized salmon aquaculture industries in Tasmania and the freshwater is released into the environment after initial use. Powell et al. [37] have suggested the use of alternative bathing techniques using hydrogen peroxide (H_2O_2), but there have been no strong initiatives undertaken to overcome the technical challenges in relation to Salmon bathing to date. In some preliminary studies undertaken by some Australian aquaculture farms, concentrations ranging

from 50% to 70% H_2O_2 were employed with mixed results with risks to both fish health and to workers handling such high concentrations. Hence, the production of stronger oxidizing agents such as, reactive hydroxyl radical ($\cdot\text{OH}$) from fairly low concentrations of H_2O_2 , as demonstrated in this study in a scalable manner could serve as an alternative, safe, rapid and low-cost approach with a view to increase the treatment efficacy of AGD as well as increasing the efficiency of existing bathing techniques. Other implications of our proposed hydroxyl radical ($\cdot\text{OH}$) production via continuous-flow photoreactor could be disinfection of swimming pool and health spa, as well as that of livestock, poultry and fisheries' effluents. Please refer to the supplementary information (SI) for more preliminary discussions on further implications of $\cdot\text{OH}$ production via continuous-flow photoreactor.

5. Conclusions

We have demonstrated in-situ and accurate measurement techniques of hydroxyl radicals ($\cdot\text{OH}$) generated via direct homogeneous photolysis of H_2O_2 in aqueous solutions using simple acid-base titration of methane sulfinic acid (MSA) derived from the reaction between $\cdot\text{OH}$ radicals and dimethylsulfoxide (DMSO). We achieved an accuracy of $\pm 6.6\%$ of NMR values via our proposed method. This demonstration has enabled us to develop a scalable production technique of hydroxyl radicals ($\cdot\text{OH}$) from low concentration H_2O_2 (ranging from 0.1 M – 5 M) using low-cost, portable and continuous-flow photoreactor in this study. Most importantly, we have established the fact that in regards to the scalability of a photoreactor system employed for the photolysis of H_2O_2 into $\cdot\text{OH}$ radical, the quantum yield of photolytic conversion in aqueous solution cannot be regarded as a linear function of H_2O_2 initial concentration. In industrial processes where high molar concentrations of H_2O_2 is employed, our proposed scalable $\cdot\text{OH}$ radical production method via continuous-flow photoreactors can be regarded as a safe, simple, accurate and cost-effective technique.

6. Acknowledgement

The authors would like to acknowledge the financial contribution of Food Innovation Australia Limited (FIAL) and Huon Aquaculture Company Limited through the Enterprise Solution Centre Program (ESCP) grant to Victoria University, Melbourne, Australia (ID: 20191009 FE CRA HuonFIAL_1107).

7. References

1. F.-C. Cheng, J.-F. Jen, T.-H. Tsai, Hydroxyl radical in living systems and its separation methods, *J. Chromatogr. B*, 781(2002)481-496.
2. B. Lipinski, (2011) Hydroxyl radical and its scavengers in health and disease, *Oxid. Med. Cell. Longev.*, 2011, 809696.
3. B. Halliwell, J.M. Gutteridge, (2015) *Free radicals in biology and medicine*, 5th ed., Oxford University Press, United Kingdom.
4. H. Shi, Y. Sui, X. Wang, Y. Luo, L. Ji, Hydroxyl radical production and oxidative damage induced by cadmium and naphthalene in liver of *Carassius auratus*, *Comparative Biochemistry and Physiology Part C: Toxicology & Pharmacology*, 140 (2005)115-121.
5. L. Diez, M.-H. Livertoux, A.-A. Stark, M. Wellman-Rousseau, P. Leroy, High-performance liquid chromatographic assay of hydroxyl free radical using salicylic acid hydroxylation during in vitro experiments involving thiols, *Journal of Chromatography B: Biomedical Sciences and Applications*, 763(2001)185-193.
6. F. Vatansever, W. C. M. A., De Melo, P. Avci et al. Antimicrobial strategies centered around reactive oxygen species - bactericidal antibiotics, photodynamic therapy and beyond, *FEMS Microbiol Rev.*, 37 (2013)955–989. doi:10.1111/1574-6976.12026
7. S. S. Shinde, C. H. Bhosale, K. Y. Rajpure, J. H. Lee, Remediation of wastewater: Role of hydroxyl radicals, *Journal of Photochemistry and Photobiology B: Biology* 141 (2014) 210–216

8. E. M. Cuerda-Correa, M. F. Alexandre-Franco, C. Fernández-González, Advanced oxidation processes for the removal of antibiotics from water. An overview, *Water*, 12(2020)102; doi:10.3390/w12010102
9. K. E. O'Shea, D. D. Dionysiou, Advanced oxidation processes for water treatment, *J. Phys. Chem. Lett.* 3(2012)2112–2113, dx.doi.org/10.1021/jz300929x
10. S., Guittonneau, J. D., Laat, J. P. Duguet et al. Oxidation of Parachloronitrobenzene in Dilute Aqueous Solution by O₃ + UV and H₂O₂ + UV : A Comparative Study *Ozone: Science & Engineering*, 12(1990)73-94.,
11. A. K. Biń, P. Machniewski, R. Sakowicz et al. Degradation of Nitroaromatics (MNT, DNT AND TNT) by AOPs, *Ozone: Science & Engineering*, 23(2001) 343-349.
12. Z. M. Li, P. J. Shea, S. D. Comfort, Nitrotoluene destruction by UV-catalyzed fenton oxidation, *Chemosphere*, 36(1998)1849–1865.
13. F. A. Momani, Impact of photo-oxidation technology on the aqueous solutions of nitrobenzene: Degradation efficiency and biodegradability enhancement, *Journal of Photochemistry and Photobiology A: Chemistry*, 179 (2006) 184-192.
14. J. D. Rodgers, N. J. Bunce, Treatment methods for the remediation of nitroaromatic explosives, *Water Research*, 35(2001)2101-2111.
15. P. Mahbub, P. N. Nesterenko, Application of photo degradation for remediation of cyclic nitramine and nitroaromatic explosives, *RSC Advances*, 6(2016)77603-77621
16. B. Liu, H.-X. Wang, Determination of atmospheric hydroxyl radical by HPLC coupled with electrochemical detection, *J Environ Sci (China)*, 20 (2008) 28-32.
17. Y.-L. Hu, Y. Lu, G.-J. Zhou, X.-H. Xia, A simple electrochemical method for the determination of hydroxyl free radicals without separation process, *Talanta*, 74 (2008) 760-765.
18. X. Liu, Z. Zhao, T. Shen, Y. Qin, Graphene/Gold nanoparticle composite-based paper sensor for electrochemical detection of hydrogen peroxide, *Fullerenes, Nanotubes and Carbon Nanostructures*, 27 (2019) 23-27.

19. R.C. Peña, V.O. Silva, F.H. Quina, M. Bertotti, Hydrogen peroxide monitoring in Fenton reaction by using a ruthenium oxide hexacyanoferrate/multiwalled carbon nanotubes modified electrode, *J. Electroanal. Chem.* 686 (2012) 1-6.
20. S. Ai, Q. Wang, H. Li, L. Jin, Study on production of free hydroxyl radical and its reaction with salicylic acid at lead dioxide electrode, *J. Electroanal. Chem.*, 578 (2005) 223-229.
21. L. Wu, Y. Yang, H. Zhang, G. Zhu, X. Zhang, J. Chen, Sensitive electrochemical detection of hydroxyl radical with biobarcode amplification, *Anal. Chim. Acta*, 756 (2012) 1-6.
22. Y. Huang, A. Sinha, H. Zhao et al. Real time detection of hazardous hydroxyl radical using an electrochemical approach, *Chemistry Select*, 4 (2019) 12507-12511.
23. H. Cheng, Y. Cao, Determination of hydroxyl radical in CuSO₄-vitamin C reaction system using capillary electrophoresis with electrochemical detection and its application in the determination of the scavenging activities of chrysanthemum, *Chinese Journal of Chromatography*, 25 (2007) 681-685.
24. S.A.J. Coolen, F.A. Huf, J.C. Reijenga, Determination of free radical reaction products and metabolites of salicylic acid using capillary electrophoresis and micellar electrokinetic chromatography, *Journal of Chromatography B: Biomedical Sciences and Applications*, 717 (1998) 119-124.
25. C. Tai, X. Gu, H. Zou, Q. Guo, A new simple and sensitive fluorometric method for the determination of hydroxyl radical and its application, *Talanta*, 58 (2002) 661-667.
26. R. Pehrman, M. Amme, C. Cachoir, Comparison of chemiluminescence methods for analysis of hydrogen peroxide and hydroxyl radicals, *Czechoslovak Journal of Physics, Suppl. D*. 56 (2006) D373-D379.
27. D. Wang, W. Yu, X. Pang, et al. A new method for hydroxyl radical detection by chemiluminescence of flue-cured tobacco extracts, *Spectrochimica Acta Part A: Molecular and Biomolecular Spectroscopy*, 204(2018)436-439

28. A.-H. Liang, S.-M. Zhou, Z.-L. Jiang, A simple and sensitive resonance scattering spectral method for determination of hydroxyl radical in Fenton system using rhodamine S and its application to screening the antioxidant, *Talanta*, 70(2006)444-448.
29. M. G. Steiner, C. F. Babbs, Quantitation of the hydroxyl radical by reaction with dimethyl sulfoxide, *Biochemistry and Biophysics*, 278(1990)478-481
30. C. F. Babbs, M. J. Gale, Colorimetric assay for methanesulfinic acid in biological samples, *Anal Biochem.* 163(1987)67-73. doi: 10.1016/0003-2697(87)90093-5
31. F. Wudl, D. A. Lightner, D. J. Cram, Methanesulfinic acid and its properties, *J. Am. Chem. Soc.*, 89(1967) 40994101.
32. D. S. Argyropoulos, H. Li, A. R. Gasper et al. Quantitative ³¹P NMR detection of oxygen-centered and carbon-centered radical species, *Bioorganic & Medicinal Chemistry* 14(2006) 4017–4028
33. C.-H. Liao, M. Gurol, Chemical Oxidation by Photolytic Decomposition of Hydrogen Peroxide, *Environ. Sci. Technol.* 29(1995)3007-3014.
34. S. Luňák, P. Sedlák, Photoinitiated reactions of hydrogen peroxide in the liquid phase, *J Photochem. Photobiol A: Chem.*, 68 (1992) 1-33
35. L. J. Heidt, The photolysis of hydrogen peroxide in aqueous solution, *J. Am. Chem. Soc.*, 54 (1932) 2840–2843.
36. D.C. Harris, Quantitative chemical analysis, Seventh ed., W. H. Freeman and Company, New York, 2007.
37. M. D. Powell, P. Reynolds, T. Kristensen, Freshwater treatment of amoebic gill disease and sea-lice in seawater salmon production: Considerations of water chemistry and fish welfare in Norway, *Aquaculture*, 448(2015)18 –28.
38. P. Mahbub, A. Sharma, Investigation of alternative water sources for fish farming using life cycle costing approach: a case study in North West Tasmania, *Journal of Hydrology*, 579 (2019) 124215

Journal Pre-proofs

Tables

Table 1 Results of spent H₂O₂ and ·OH radical produced from various starting concentrations of H₂O₂ by different layers of the photoreactor system with fixed flowrate of 20 mL/min (results illustrating average ± standard deviation of three replicate samples)

H ₂ O ₂ initial Concentration (M), average ± st.dev	H ₂ O ₂ remaining (M), average ± st.dev	H ₂ O ₂ Spent (M), average ± st.dev	Layer	·OH produced (M), average ± st.dev
10.48±0.002	5.32±0.002	5.16±0.01	1	0.018±0.002
10.48±0.01	3.3±0.01	7.18±0.002	2	0.024±0.002
10.48±0.002	3.7±0.002	6.78±0.002	3	0.025±0.01
10.48±0.01	3.6±0.01	6.88±0.01	4	0.029±0.001
9.44±0.004	5.3±0.01	4.13±0.01	1	0.013±0.004
9.44±0.01	3.5±0.001	5.94±0.001	2	0.02±0.001
9.44±0.01	3.8±0.01	5.64±0.011	3	0.023±0.004
9.44±0.002	3.8±0.002	5.64±0.002	4	0.024±0.002
10.48±0.002	3.1±0.002	7.38±0.002	3+2	0.0375±0.00 4
10.48±0.003	2.05±0.001	8.43±0.001	3+2+ 1	0.045±0.01
5±0.002	3.55±0.001	1.45±0.001	3+2+ 1	0.043±0.004
7.515±0.002	5.15±0.001	2.366±0.001	3+2+ 1	0.045±0.000 1
5±0.01	3.11±0.01	1.9±0.01	4+3+ 2+1	0.055±0.01
1±0.002	0.81±0.004	0.2±0.004	4+3+ 2+1	0.074±0.004
0.5±0.002	0.445±0.01	0.055±0.01	4+3+ 2+1	0.0834±0.00 01
0.1±0.003	0.089±0.001	0.011±0.001	4+3+ 2+1	0.042±0.01

Table 2 Comparison between acid-base titration method and NMR method for $\cdot\text{OH}$ radical

determination in aqueous solution

Initial Reading of titration, V1, mL	Final Reading of titration, V2, mL	Dilution Factor, DL	Sample volume		$\cdot\text{OH}$ radical concentrations via titration (=DL x 0.001x(V2-V1)/V3, mM)	Ratio of 2.42 mM TMP(I.S.)/DIPPMPO-OH adduct via NMR, R1	$\cdot\text{OH}$ radical concentrations via NMR (=2.42/R1), mM
			Titration, V3, mL	NMR, V4 (= 0.2 mL OH+0.2 mL D2O+0.1 mL CrCl ₃)			
18.3	18.8	6	3	0.5	1	2.398	1.009
18.8	19.3	6	3	0.5	1	2.394	1.011
19.3	19.9	6	3	0.5	1.2	2.421	0.999
21.0	21.6	7	3.5	0.5	1.2	2.38	1.017
21.6	22.1	7	3.5	0.5	1	2.353	1.028
					Titration mean \pm st.dev = 1.08 \pm 0.11	NMR mean \pm st.dev = 1.0128 \pm 0.01	

Table 3 Comparison amongst $\cdot\text{OH}$ radical detection platforms and detection methods

Detection platform (detection method)	$\cdot\text{OH}$ source + trapping agents	$\cdot\text{OH}$ production mode	Flow rate [$\mu\text{L min}^{-1}$]	Linearity [$\mu\text{M} - \text{mM}$]	^a LOD [nM]	Ref.
Continuous-flow photoreactor (Acid-base titration)	$\text{H}_2\text{O}_2 + \text{UV} + \text{DMSO}$	Continuous	20000	500 – 100	500000	This work
EC (SWV)	Fenton reaction + DNA-Au NPs	Batch	-	3 – 10	3000	[21]
HPLC (GCE, AD)	Fenton reaction + Salicylic acid	Batch	-	0.06 – 0.001	13-20	[5]
Electron spin resonance	Fenton reaction + PBN	Batch	-	Not reported	Not reported	[4]
Resonance scattering	Fenton reaction + Iodine + Rhodamine	Batch	-	0.09 – 0.01	40	[28]
MECC (UV)	Fenton reaction + Salicylic acid	Batch	-	1 – 0.1	200	[24]

^a LOD = Limits of Detection; three times standard deviations (3SD) of a blank response (noise level)/slopes of the corresponding calibration curves [36].
 amperometric detection (AD), square wave voltammetry (SWV), dimethyl sulfoxide (DMSO), electrochemical (EC), glassy carbon electrode (GCE), phenyl-tert-butyl nitron (PBN), micellar electrokinetic capillary chromatography (MECC), DNA-Au nanoparticles (DNA-Au-Nps).

Figures and Figure Captions

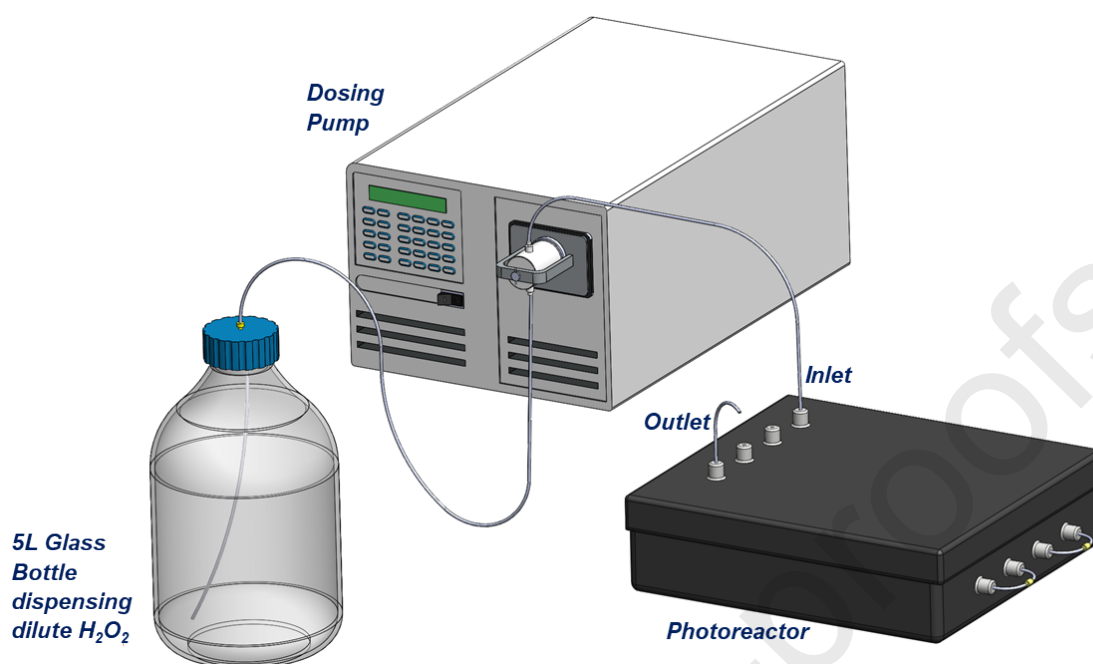


Figure 1 The proposed laboratory-scale scheme of the continuous-flow photoreactor system

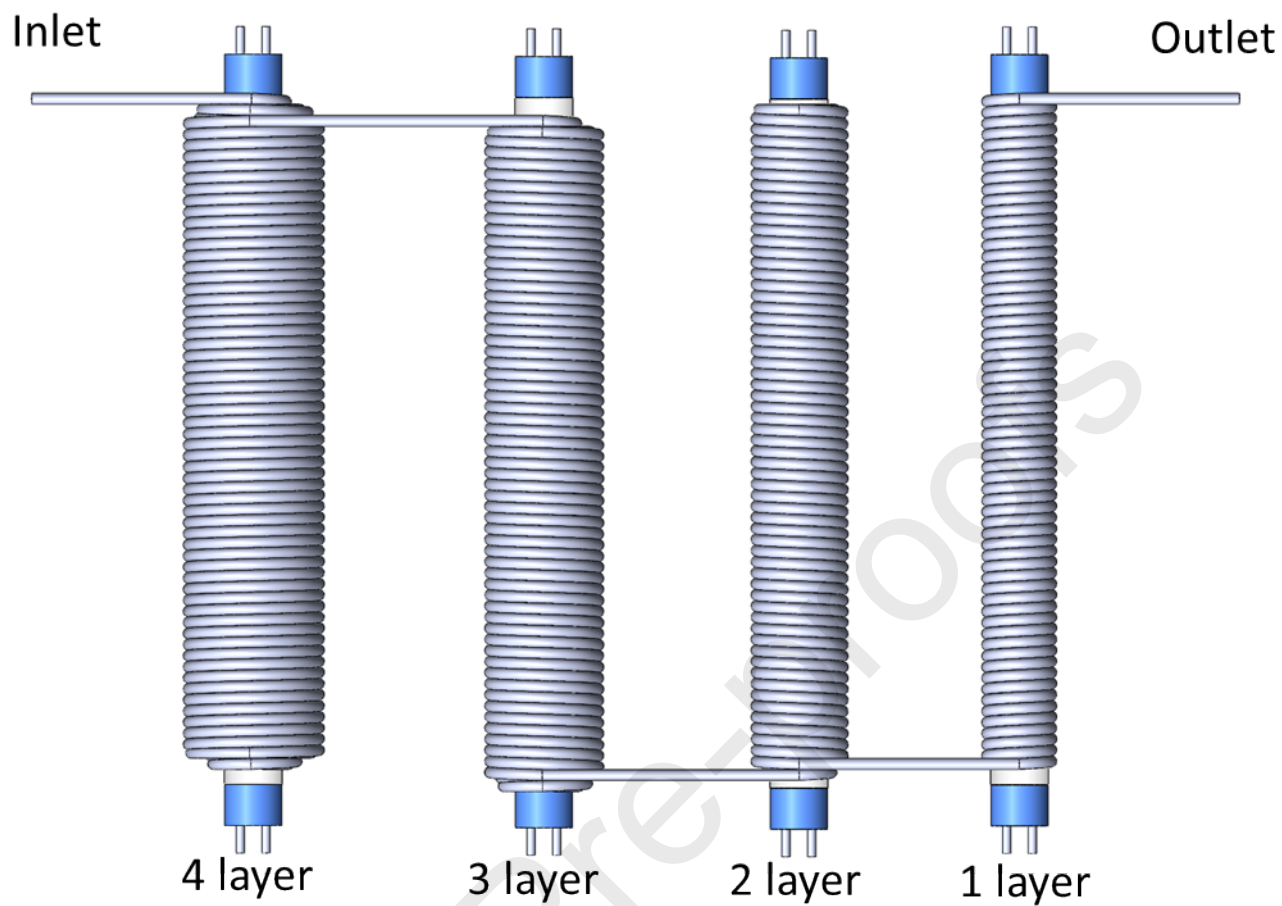


Figure 2a Schematic top-view of serially connected layers (i.e., 4+3+2+1) of the reactor system

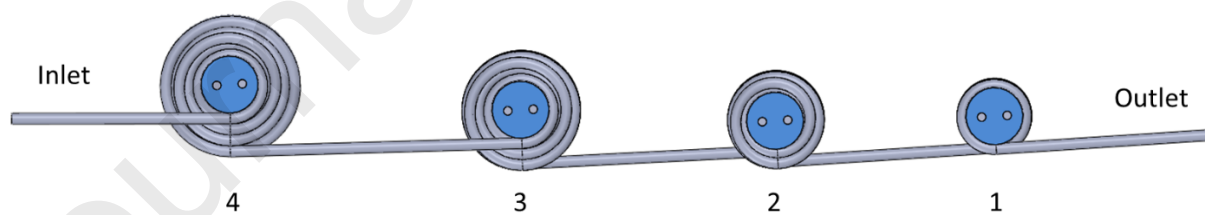


Figure 2b Schematic side elevation-view of serially connected layers (i.e., 4+3+2+1) of the reactor system

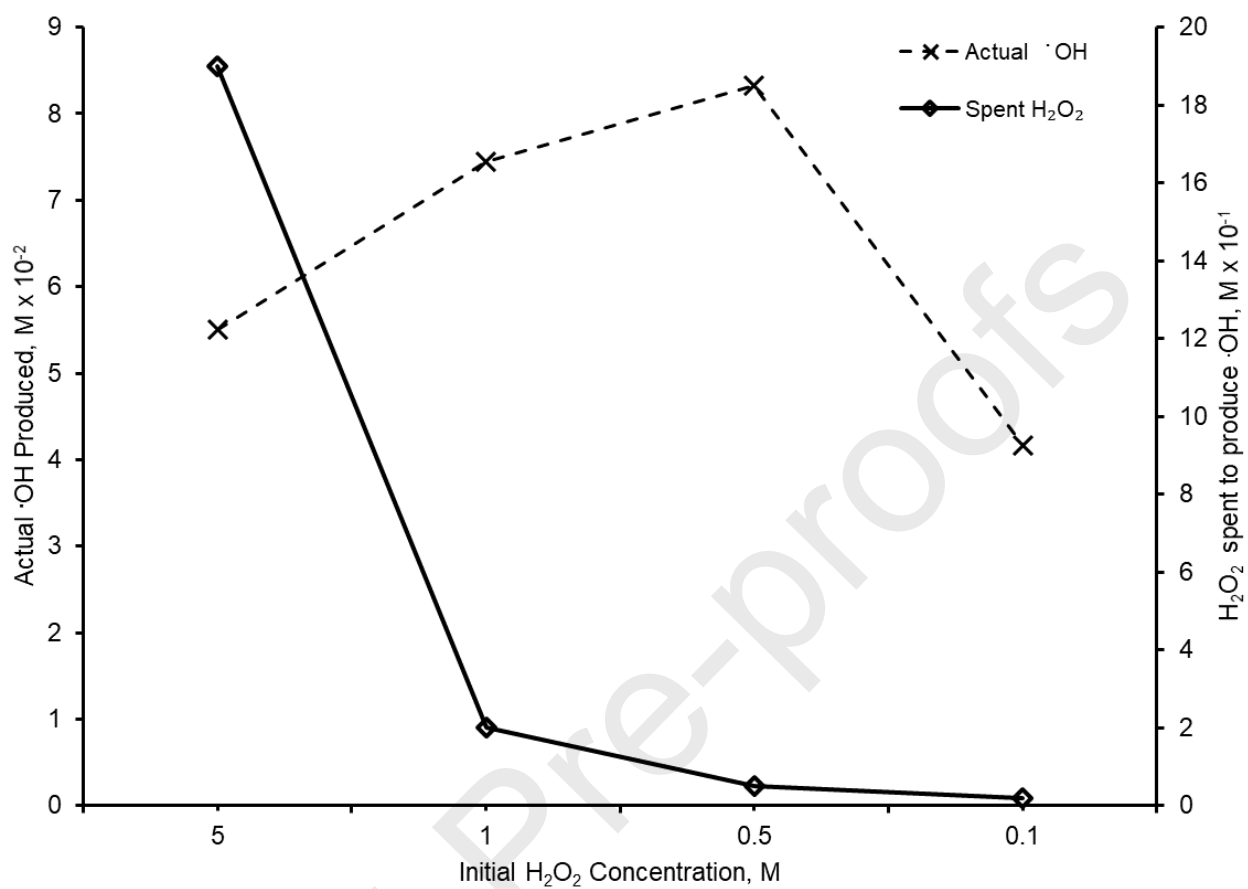


Figure 3A the non-linear relation between spent H_2O_2 and $\cdot\text{OH}$ radical produced by (4+3+2+1)

photoreactor at fixed flow rate 20 mL/min and fixed optical path-length

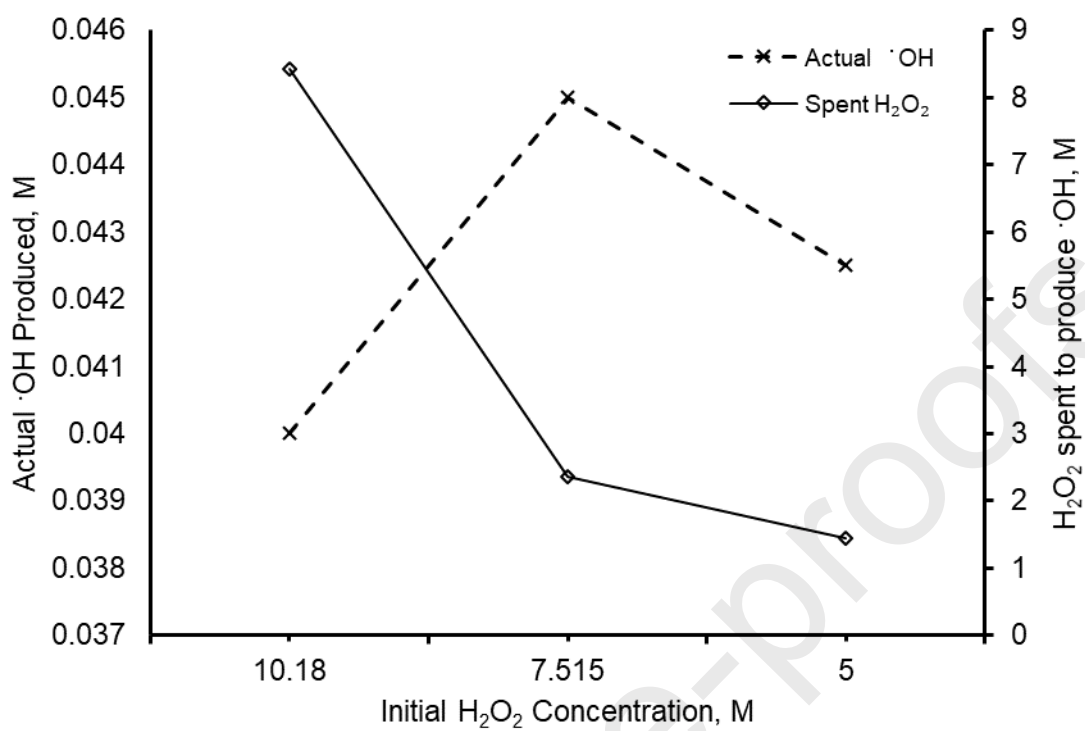


Figure 3B the non-linear relation between spent H₂O₂ and ·OH radical produced by (3+2+1) photoreactor at fixed flow rate 20 mL/min and fixed optical path-length

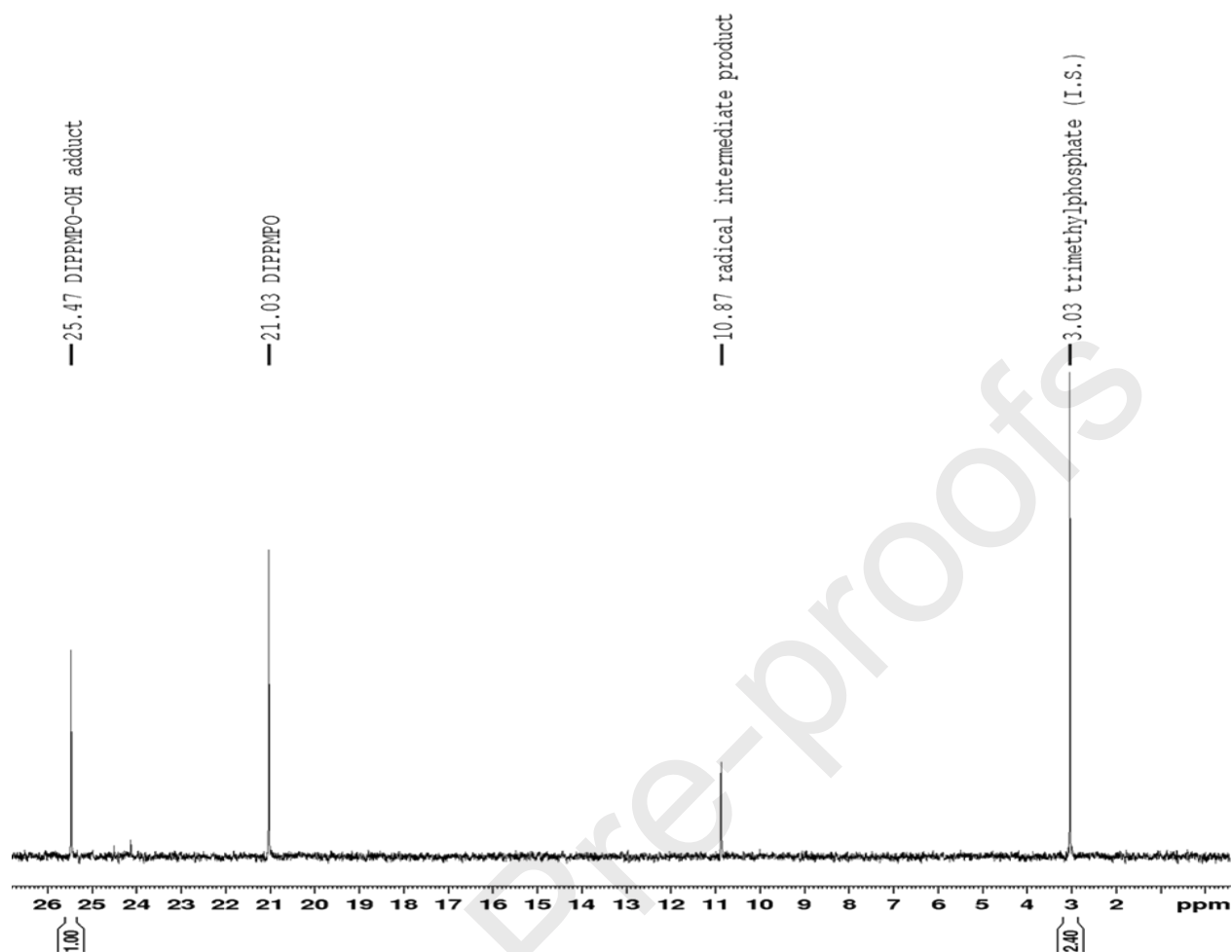
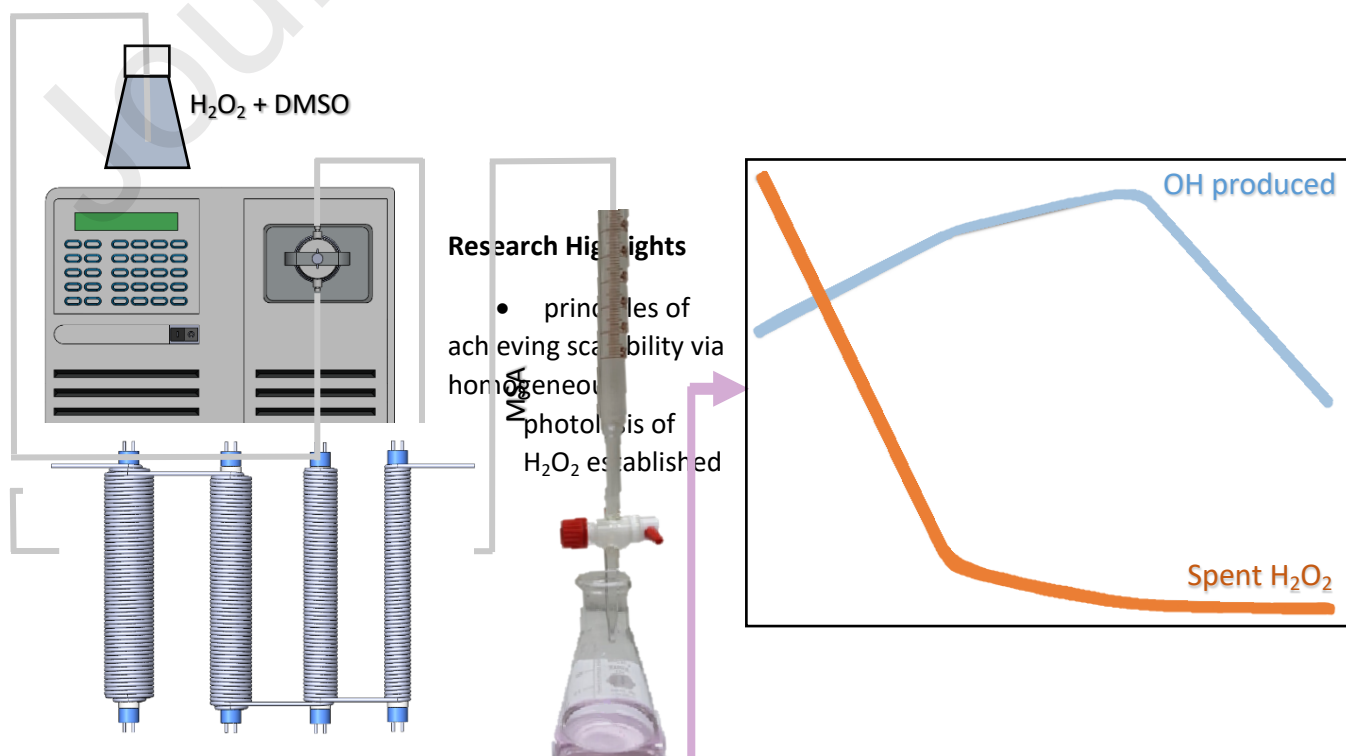


Figure 4 Quantitative ^{31}P NMR spectra of the products formed from the UV photolysis of H_2O_2 in aqueous solution, I.S. (internal standard) = trimethylphosphate (TMP); Ratio of 2.42 mM TMP(I.S.)/DIPPMPPO-OH adduct via NMR = 2.40



- quantum yield of photolytic conversion is not a linear function of H_2O_2 concentration
- *in-situ* hydroxyl ($\cdot\text{OH}$) radical measurement technique verified by NMR

Journal Pre-proofs